Journal of Power Sources 195 (2010) 1479–1485

Contents lists available at ScienceDirect

Journal of Power Sources

journal homepage: www.elsevier.com/locate/jpowsour

Polyfluorinated boron cluster-based salts: A new electrolyte for application in $Li_4Ti_5O_{12}/LiMn_2O_4$ rechargeable lithium-ion batteries

C.M. Ionica-Bousquet[a,1], D. Muñoz-Rojas[a,2], W.J. Casteel[b], R.M. Pearlstein[b,*], G. GirishKumar[b], G.P. Pez[b], M.R. Palacín[a]

[a] Institut de Ciència de Materials de Barcelona, CSIC, Campus UAB, E-08193 Bellaterra, Spain
[b] Air Products and Chemicals, Inc., 7201 Hamilton Blvd., Allentown, PA 18195, USA

ARTICLE INFO

Article history:
Received 17 July 2009
Received in revised form
11 September 2009
Accepted 11 September 2009
Available online 20 September 2009

Keywords:
Titanate
Manganate
Spinel
Dodecaborate
Fluorinated

ABSTRACT

The cycling performance of $Li_4Ti_5O_{12}$ and $LiMn_2O_4$ electrode materials has been studied in half and complete Li-ion cells with two new polyfluorinated boron cluster lithium salts ($Li_2B_{12}F_xH_{12-x}$) as the electrolytes. The results were compared with those obtained for the standard electrolyte, 1 M $LiPF_6$ dissolved in ethylene carbonate and dimethyl carbonate (EC:DMC; 1:1, v/v). Three different technologies were employed for electrode fabrication: powder mixture, self-standing films and films deposited on the current collector. The latter exhibit the most interesting behavior and best performance. Cells assembled using the new electrolyte salts show excellent reversibility, coulombic efficiency, rate capability and cyclability comparable with the standard electrolyte. These features confirm the feasibility of using these polyfluorinated boron cluster-based salts as new stable Li-ion battery electrolytes.

1. Introduction

Lithium-ion batteries are now the most advanced technology for rechargeable power in portable electronics and are used in a myriad of devices such as cellular phones, laptop computers, organizers, cameras, etc. Since first being commercialized in Japan by Sony in 1991 [1], Li-ion batteries have improved in performance, reliability and safety. This has created opportunities for new applications in areas such as transportation (electric and hybrid cars), space (satellites) [2] and medicine (implantable devices) [3,4].

The cycle life of a rechargeable Li-ion battery depends on the long-term reversibility of the cell chemistries. A critical factor in maintaining this reversibility is the electrochemical and chemical stability of the electrolyte, a requirement which is often disregarded. Various kinds of salts have been utilized as solute in both liquid- and gelled-type electrolytes for lithium batteries. These salts include $LiClO_4$ [5,6], $LiMF_x$ (M = B, P, As and x = 4 or 6) [7,8], $LiCF_3SO_3$ (LiTf) [9,10], $LiN(CF_3SO_2)_2$ (LiTFSI) [11,12], $LiN[(C_2F_5SO_2)_2]$ (LiBETI) [13–16], and LiBOB [17,18]. With the exception of $LiClO_4$ and LiBOB, all of the salts have fluorinated anions. These electrolytes salts are, in general, highly soluble in aprotic solvents such as ethylene carbonate (EC), propylene carbonate (PC), dimethyl carbonate (DMC), or mixtures of them, and provide high ionic conductivities [19].

Recently, polyfluorinated boron cluster salts, such as lithium polyfluorododecaborates ($Li_2B_{12}F_xZ_{12-x}$ wherein $x \leq 12$ and Z = H, Cl or Br) [20–23], have been developed for use as electrolyte salts. These new electrolytes offer several putative advantages such as high electrochemical, thermal, and hydrolytic stability, as well as the possibility of using low salt concentration. Another important feature of these salts is their ability to provide intrinsic protection against overcharge through redox-shuttle chemistry [21].

Such a system could greatly simplify the sophisticated protection circuitry currently in every cell of a battery pack. Indeed, in view of a recent battery manufacturers' recall of millions of lithium-ion cells for laptop computers, the need for safer, alternative material has re-emerged not only for electrode materials but also electrolyte salts and solvents.

The primary objectives of this study were to measure the performance and stability of this new family of electrolyte salts, and to assess the feasibility of applying them in rechargeable Li-ion systems (as compared to standard electrolytes). This report presents tests results for two of these new boron cluster-based salts: $Li_2B_{12}F_{12}$, a single-component salt; and $Li_2B_{12}F_8H_4$, a salt

* Corresponding author at: Air Products and Chemicals, Inc., Global Technology Center, 7201 Hamilton Blvd., Allentown, PA 18195, USA. Tel.: +1 610 481 8594; fax: +1 610 706 7151.
E-mail address: pearlsrm@airproducts.com (R.M. Pearlstein).
[1] Present address: AIME-ICG, Université Montpellier II, CC1502, Place E. Bataillon, 34095 Montpellier Cedex 5, France.
[2] Present address: Department of Materials Science and Metallurgy, University of Cambridge, Pembroke St., Cambridge CB2 3QZ, UK.

0378-7753/$ – see front matter © 2009 Elsevier B.V. All rights reserved.
doi:10.1016/j.jpowsour.2009.09.023

mixture with that average composition. Electrolyte solutions were evaluated in both half and full Li-ion cells. Stability, cyclability and coulombic efficiency were measured for these cells. In view of their current stage of commercial development, $Li_4Ti_5O_{12}$ and $LiMn_2O_4$ were selected as electrode materials to evaluate based on their safer operation voltage, price and non-toxicity. In order to ensure that test results were independent of the chosen electrode fabrication method and to detect any compatibility problem with ordinary electrode components, three differing technologies were used to make the $Li_4Ti_5O_{12}$ electrodes. All tests were also repeated with a standard electrolyte solution as a control.

2. Experimental

2.1. Materials synthesis, structural and morphological characterization

The two electrolyte salts, $Li_2B_{12}F_{12}$ and $Li_2B_{12}F_8H_4$, were prepared and purified as reported elsewhere [20]. Stoichiometric $LiMn_2O_4$ was synthesized by heating a stoichiometric mixture of Li_2CO_3 (99%, Aldrich) and electrochemically prepared manganese dioxide (EMD) in air at 800 °C for 72 h, with two intermediate grindings and a final slow cooling (20 °C h^{-1}) [24,25].

$Li_4Ti_5O_{12}$ was prepared as reported elsewhere [26,27] by dispersing stoichiometric amounts of TiO_2 (<5 μm, 99.9%, Aldrich) and Li_2CO_3 (99%, Aldrich) in a mixture of alcohol/deionized water/sugar (99%, Alfa Aesar). These components were combined using a weight ratio of 3.3:1.3:1. After the solvent was removed, the resulting powder was ground and heat-treated in air at 750 °C for 12 h to decompose the Li_2CO_3, and then at 850 °C for 24 h. Several techniques were used to characterize the resulting oxide powders. The phase purity was assessed through X-ray powder diffraction (XRD) by using a Rigaku Rotaflex Ru-200B Spectrometer with Cu Kα radiation source (λ = 0.15418 nm). Cell parameters were refined with the program FULLPROF [28].

Grain morphology and particle size were determined by scanning electronic microscopy (SEM) using a Philips 515 with 5 nm resolution (which can be operated between 0.2 and 30 kV). The specific surface area of the prepared sample was measured by N_2 gas adsorption and desorption (Micrometrics ASAP 2000) using the Brunauer–Emmett–Teller (BET) method.

2.2. Electrode preparation and battery assembly

Electrochemical experiments were performed using two-electrode Swagelok™ cells [29]. Three different fabrication methods were used to prepare the electrodes. In all trials, cells were made and tested at the same time as the two test electrolytes and the control to ensure that external parameters (e.g., diurnal temperature variations in the test room) were identical for the different electrolytes. The first method, known as "powder," consists of mixing a sample of oxide powder ($Li_4Ti_5O_{12}$ or $LiMn_2O_4$) with 15 wt% SP Carbon (kindly supplied by MMM, Belgium). The loading of active material was in the range of 8–10 mg.

The second method, referred to as "PTFE", allows the manufacture of self-standing electrodes by preparing a mixture of 85 wt% oxide powder, 10 wt% acetylene black carbon powder and 5 wt% polytetrafluoroethylene (PTFE) binder (60% PTFE dispersed in water, Aldrich). The resulting paste was spread into 5 cm × 10 cm sheets about 35 μm thick, from which 0.95 cm^2 circular electrodes were cut. The electrodes were vacuum-dried at 120 °C prior to use. The typical loading of active material was in the range of 20–30 mg cm^{-2}.

Alternatively, "cast" electrodes were obtained by doctor-blade coating a slurry containing 84 wt% oxide powder, 8% acetylene black powder and 8 wt% binder (polyvinylidene difluoride, PVDF) dissolved in N-methylpyrrolidone (NMP) onto the current collector. The current collector was 18 μm thick copper foil (GoodFellow). Circular 0.95 cm^2 electrodes were cut and also dried at 120 °C in vacuum prior to use. The typical loading of active material was in the range of 3–5 mg cm^{-2}. The thickness of the dried electrodes was 15–20 μm, these electrodes were thinner and thus suitable for higher rate cycling (C/2).

Two sheets of Whatman GF/D borosilicate glass fiber, used as a separator, were soaked with electrolyte. Three electrolyte solutions were used: 0.4 M $Li_2B_{12}F_{12}$ in ethylene carbonate/dimethylcarbonate (EC/DMC 1:1 volume), 0.4 M $Li_2B_{12}F_8H_4$ in EC/DMC (1:1 volume) and 1 M $LiPF_6$ in EC/DMC (1:1 volume; Merck Battery Grade). The first two of these, new salts evaluated in this study, are referred to as "BF" and "BFH", respectively. The last electrolyte solution is denoted as "standard".

Lithium half cells were assembled with either $Li_4Ti_5O_{12}$ or $LiMn_2O_4$ as working electrodes, and Li metal foil (0.38 mm thick, Aldrich) as a counter electrode. In full Li-ion cells, balanced amounts of $Li_4Ti_5O_{12}$ and $LiMn_2O_4$ were used as the respective negative and positive electrodes. The specific capacity and rate of the full battery were always referred to the mass of the positive electrode.

The cells were charged and discharged in different potential windows (depending on the case) at various C-rate regimes between C/2 and C/20 by using a VMP Potentiostat/Galvanostat (Bio-Logic) operating in a galvanostatic mode. All tests were performed at room temperature.

3. Results and discussion

3.1. Materials characterization

The XRD pattern of the prepared $LiMn_2O_4$ sample (Fig. 1a) exhibits the characteristic diffraction peaks of the $LiMn_2O_4$ phase (refined cell parameter: a = 0.82336(2) nm) (JCPDS file no. 35-0782), with perhaps a very slight amount of Li_2MnO_3 impurity. A typical SEM micrograph is shown in Fig. 1b, where it can be seen that the product is composed of fine submicron primary particles that form 10–15 μm agglomerates. The measured BET surface area is 12 m^2 g^{-1}.

The XRD pattern of the prepared $Li_4Ti_5O_{12}$ sample is shown in Fig. 2a. The main diffraction peaks of the $Li_4Ti_5O_{12}$ spinel phase are present, along with some minor extra diffraction peaks at 2θ = 27.4°, 37.3° and 54.3° that are attributed to the presence of a small amount of rutile-phase TiO_2. The refined lattice parameter of $Li_4Ti_5O_{12}$ is a = 0.83562(2) nm, which is consistent with results reported by Ohzuku et al. [30]. The synthesis employed here allows the preparation of homogeneous compounds with finer particle sizes, as the decomposition of the added sugar during heat treatment inhibits particle agglomeration. The SEM micrograph in Fig. 2b shows typical 0.8–1 μm particles. The measured BET surface area is 8 m^2 g^{-1}.

3.2. Electrochemical analysis

3.2.1. Half cell tests

To isolate potential electrode manufacturing or electrolyte compatibility problems, all $LiMn_2O_4$ and $Li_4Ti_5O_{12}$ electrodes were first individually tested in lithium half cells with the new BF and BFH solutions as well as the standard $LiPF_6$ electrolyte.

Fig. 3a–c shows the voltage vs. composition profiles for galvanostatic tests of $LiMn_2O_4$ electrodes (PTFE Technology) in the 4.3–3.8 V voltage range at C/20. Two large, well-known and reversible plateaus [31,32] – at 4.05 and 4.1 V upon lithium extraction/reinsertion – are observed in the curves for all three electrolyte salts. Relatively similar reversible capacities, such as

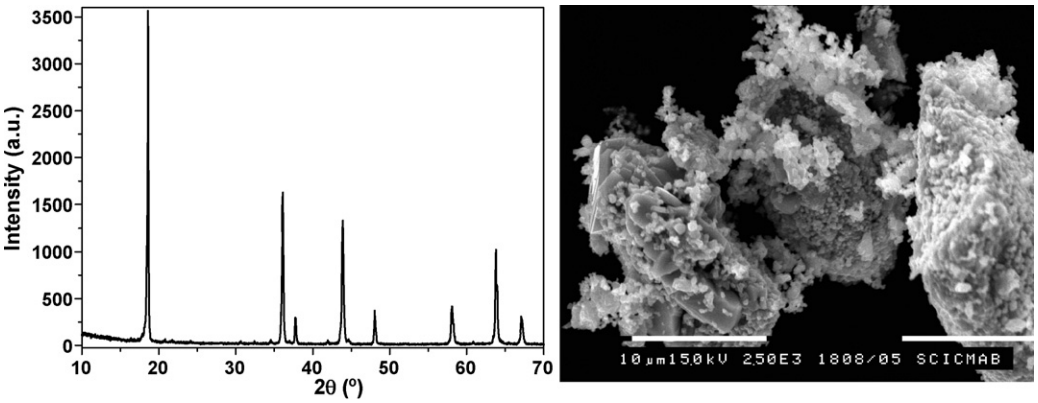

Fig. 1. XRD pattern (a) and SEM micrographs (b) of the $LiMn_2O_4$ spinel.

110–120 mAh g^{-1}, are in close agreement with the usual values reported under these conditions [21]. Polarization values are slightly different (80 mV being the largest and 45 mV the smallest) and increase in the sequence: standard < BF < BFH. This variation can be explained by differences in the conductivity of these solutions attributed to their slightly higher viscosity and lower degree of dissociation, or by differences in interfacial capacitance for each of these salts [22].

However, the most significant difference is observed for the BFH electrolyte, for which a higher capacity is observed during the first oxidation. The overall stability of the electrodes can be deduced from the capacity vs. cycle number plot (Fig. 4), from which excellent coulombic efficiency can be inferred. Indeed, the fact that the extra capacity delivered by the cell with BFH electrolyte upon the first oxidation is mostly irreversible results in capacity values very similar to those for cells using BF and standard electrolytes after 10 cycles. This additional, largely irreversible capacity is therefore likely related to some irreversible oxidation of low-fluorination components of the BFH anion mixture, such as $Li_2B_{12}F_4H_8$ and $Li_2B_{12}F_5H_7$, which can occur within the voltage range of this test. As already stated, the effect of electrode technologies (powder, PTFE and cast) on the electrochemical properties and cycling performance of $Li_4Ti_5O_{12}$ cells was studied. In all cases, half cells prepared using BF, BFH and the standard $LiPF_6$ salts were tested in the voltage range between 1.2 and 1.9 V. Figs. 5 and 6 show the performance of powder electrodes consisting of a simple mixture of the active material and SP carbon; Figs 7 and 8, and 9 and 10 correspond to PTFE and cast electrode technologies, respectively. As previously explained, the later electrode technology was considered more suitable for higher rate cycling, and tests were carried out at C/2.

The observed voltage-composition profiles of $Li_4Ti_5O_{12}$ are similar in all cases (all electrode fabrication methods, electrolyte salts and rates) and evolve consistently with the well-known insertion mechanism involving a phase transition. During discharge, the voltage quickly drops to below 1.8 V and decreases steadily to a flat operating voltage of about 1.50–1.55 V. This plateau corresponds to the reversible two-phase transition. As with $LiMn_2O_4$, polarization values are slightly different, being smaller for the standard $LiPF_6$ electrolyte. Again, this variation is probably due to the higher viscosity or lower conductivity of BF and BFH electrolytes. The maximum value observed for cast electrodes with BFH electrolytes, 85 mV, is very close to the value observed for $LiMn_2O_4$. In these titanate half cells, however, no supplementary redox process is observed for any of the electrolytes tested. This indicates that no oxidizable or reducible species are active in the voltage window tested. In all cases, the capacity of the voltage plateau accounts for about 90% of the overall discharge capacity.

The values for initial capacity (first reduction) and coulombic efficiency (calculated taking the capacity on the second charge as reference) are given in Table 1. These results fall within the expected range [29] and seem to be much more dependent on the electrode technology than on the electrolyte used. In all cases, very similar values are obtained for the three electrolytes. The highest capacity is delivered by cast electrodes, which have the same surface area but much lower electrode load; the lowest capacity is delivered by PTFE self-standing films, which are thicker and have higher loading. This fact can be simply explained by the differences in current density, which, even for the lower rates used, is much higher for PTFE electrodes (0.2 mA cm^{-2}, as compared to 0.08 mA cm^{-2} for cast and 0.1 mA cm^{-2} as a mean value for

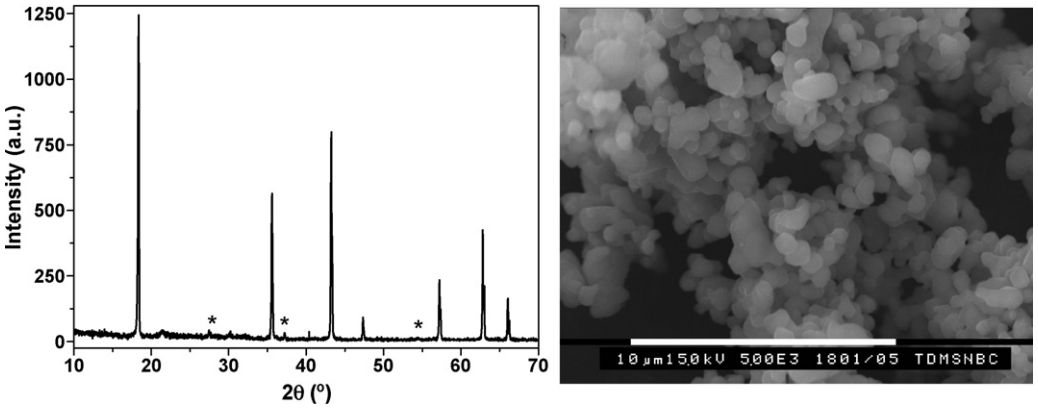

Fig. 2. XRD pattern (a) and SEM micrographs (b) of the $Li_4Ti_5O_{12}$ spinel, (*) rutile TiO_2.

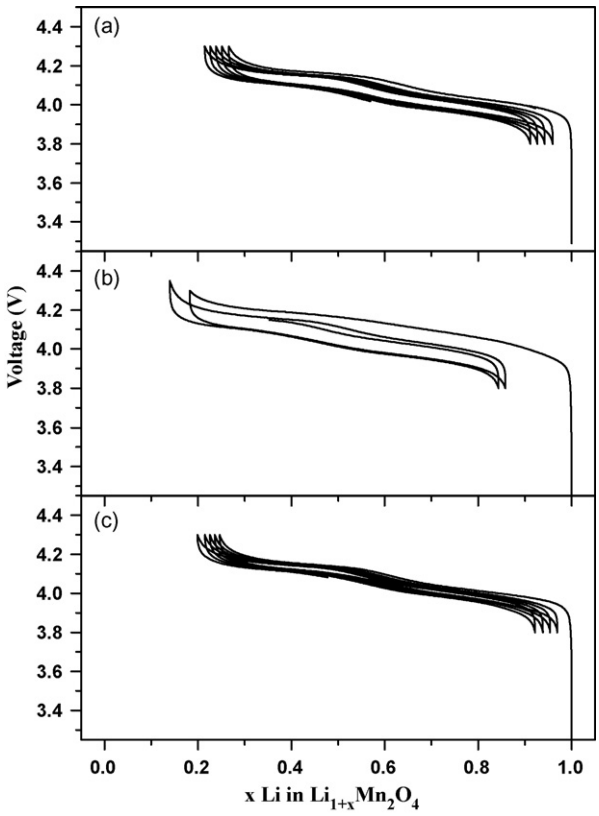

Fig. 3. Voltage vs. composition profiles obtained for $LiMn_2O_4$ (PTFE) electrode in half cells cycled at C/20 rate using (a) BF, (b) BFH, and (c) standard electrolytes.

powder). Cycling experiments thus demonstrate that the excellent capacity values are, in all cases, retained upon cycling. Again, the high coulombic efficiency upon cycling indicates that all electrodes are highly stable, and no degradation was observed for any of the electrolytes tested.

While the electrochemical performance is roughly similar in all cases and no particular compatibility problems with electrode constituents were detected, more detailed investigation reveals several small possible differences. Indeed, capacity values are always somewhat higher for BF electrolyte than for the standard $LiPF_6$ salt, a trend that was observed for all three electrode technolo-

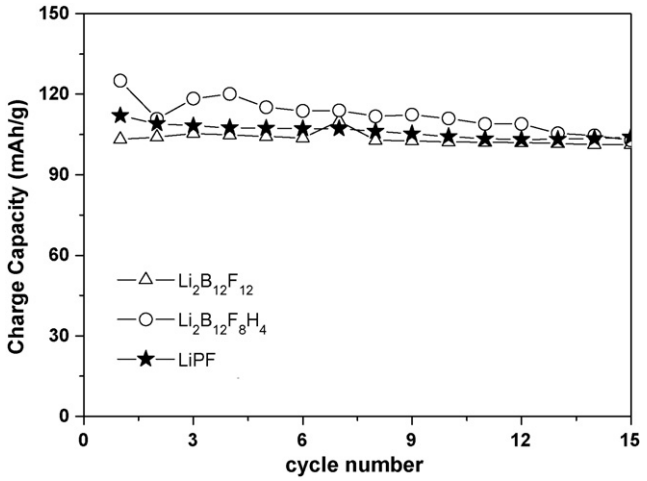

Fig. 4. Comparison of cycling behavior of lithium cells prepared using $LiMn_2O_4$ (PTFE) electrode and different electrolytes: BF, BFH, and standard $LiPF_6$. Charge/discharge rate: C/20.

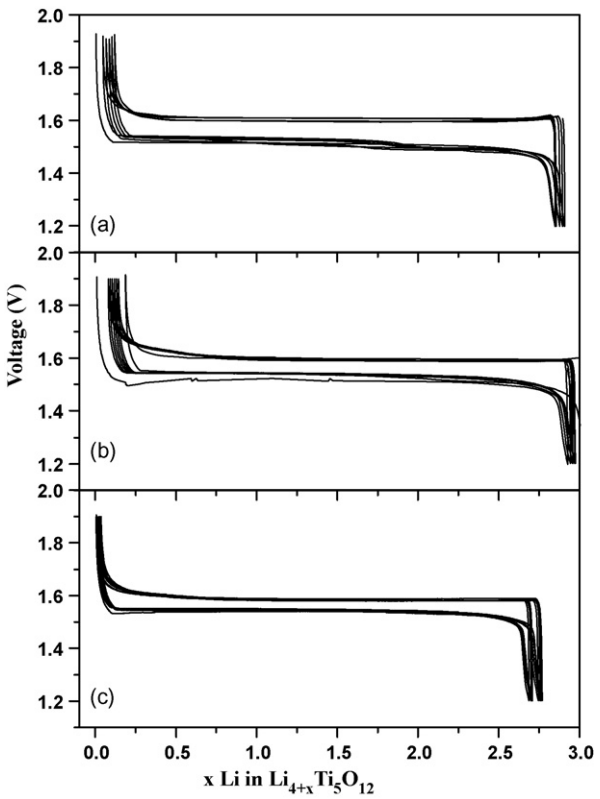

Fig. 5. Voltage vs. composition profiles obtained for $Li_4Ti_5O_{12}$ (powder) electrode in half cells cycled at C/5 rate using (a) BF, (b) BFH, and (c) standard electrolytes.

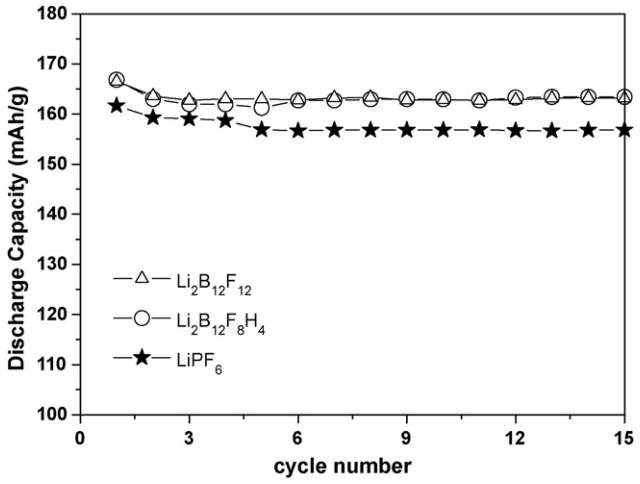

Fig. 6. Comparison of cycling behavior of lithium cells prepared using $Li_4Ti_5O_{12}$ (powder) electrode and different electrolytes: BF, BFH, and standard $LiPF_6$. Discharge/charge rate: C/5.

Table 1
Initial capacity and coulombic efficiency of $Li/Li_4Ti_5O_{12}$ half cells.

Electrode-rate	Electrolyte	Initial capacity ($mAh\,g^{-1}$)	Coulombic efficiency (%)/cycle number
Powder-C/5	BF	167	99/15
	BFH	167	100/15
	Standard	161	98/15
PTFE-C/5	BF	159	99/15
	BFH	151	99/15
	Standard	157	99/15
Cast-C/2	BF	174	100/40
	BFH	171	98/25
	Standard	171	98/40

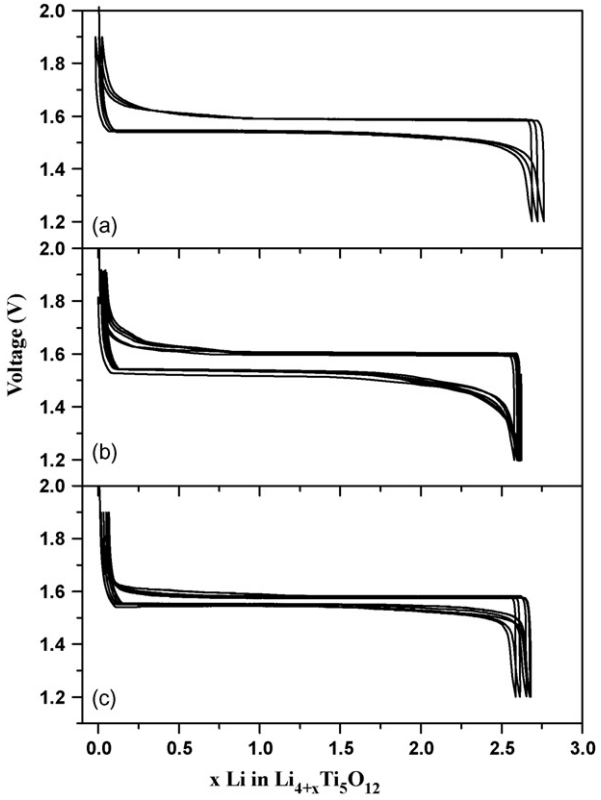

Fig. 7. Voltage vs. composition profiles obtained for $Li_4Ti_5O_{12}$ (PTFE) electrode in half cells cycled at C/5 rate using (a) BF, (b) BFH, and (c) standard electrolytes.

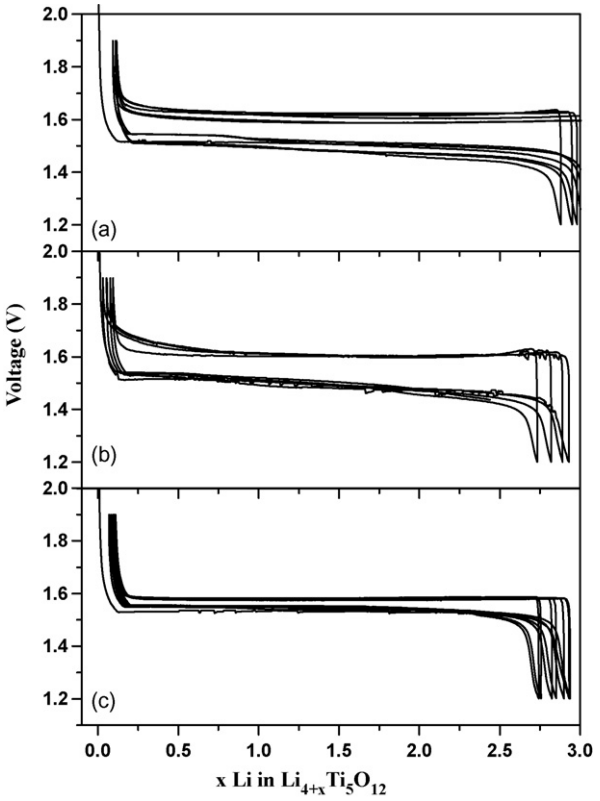

Fig. 9. Voltage vs. composition profiles obtained for $Li_4Ti_5O_{12}$ (cast) electrode in half cells cycled at C/2 rate using (a) BF, (b) BFH, and (c) standard electrolytes.

gies and which is maintained upon repeated cycling. Conversely, the capacity and efficiency delivered by the BFH electrolytes seem to be less consistent. While comparable to the capacity and efficiency of the standard $LiPF_6$ for the cast and PTFE electrodes, the BFH electrolytes perform more closely with the BF electrolytes for powder electrodes.

3.2.2. Test in full cells

Once the performance of individual electrodes in half lithium cells had been established, assembly of full $Li_4Ti_5O_{12}$/BF, BFH or $LiPF_6$ standard/$LiMn_2O_4$ lithium-ion cells was considered. Both PTFE and cast electrode technologies were tested in view of their industrial interest. It should be noted that, while PTFE technology allowed suitable cell balancing between $Li_4Ti_5O_{12}$ and $LiMn_2O_4$ by adjusting the composition and thickness of the slurries used for electrode preparation, this was not the case for cast electrodes. Indeed, the thickness of $LiMn_2O_4$ cast electrodes required to balance cast $Li_4Ti_5O_{12}$ could not be prepared while still maintaining proper adhesion. Under these circumstances, it was decided to directly adopt $LiMn_2O_4$ powder electrode technology to balance the $Li_4Ti_5O_{12}$ cast electrodes. The voltage window for these full Li-ion cell tests was adjusted according to the electrochemical window of

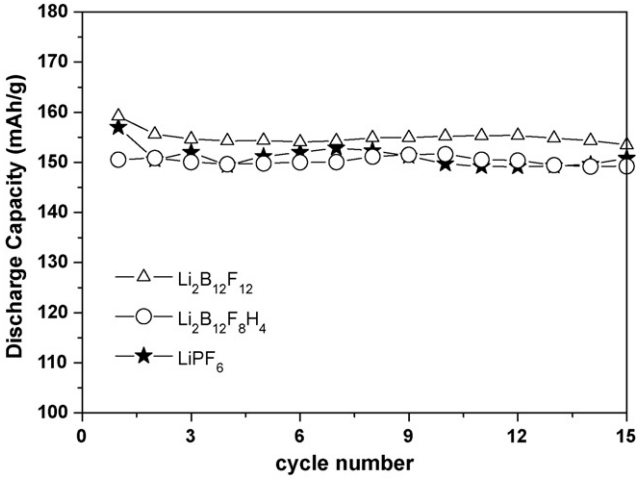

Fig. 8. Comparison of cycling behavior of lithium cells prepared using $Li_4Ti_5O_{12}$ (PTFE) electrode and different electrolytes: BF, BFH, and standard $LiPF_6$. Discharge/charge rate: C/5.

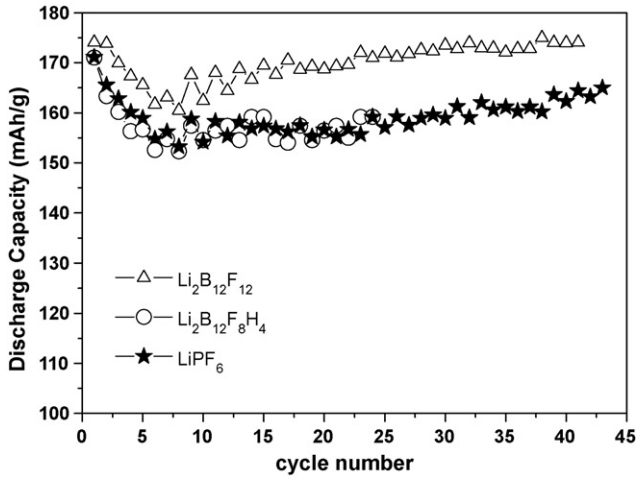

Fig. 10. Comparison of cycling behavior of lithium cells prepared using $Li_4Ti_5O_{12}$ (cast) electrode and different electrolytes: BF, BFH, and standard $LiPF_6$. Discharge/charge rate: C/2.

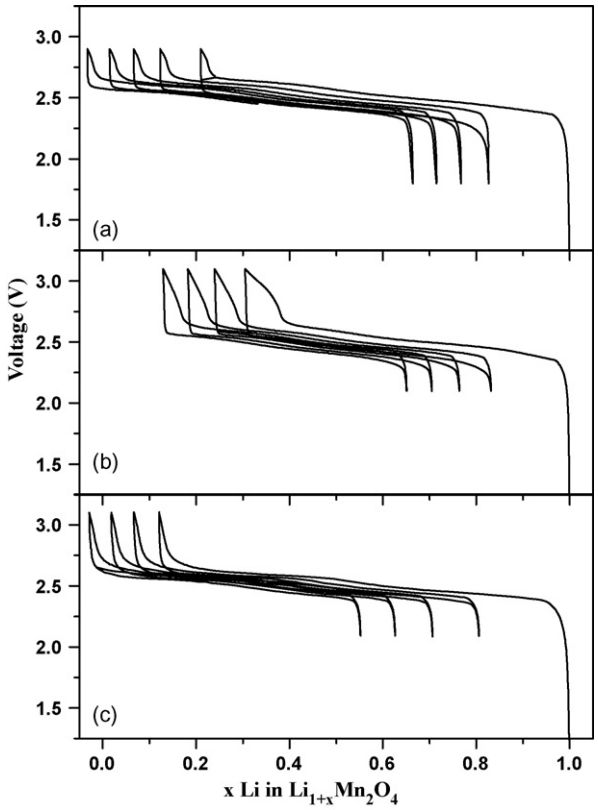

Fig. 11. Charge–discharge curves for $Li_4Ti_5O_{12}$ (cast)//$LiMn_2O_4$ (powder) full cells cycled at C/20 rate using (a) BF, (b) BFH, and (c) standard electrolytes.

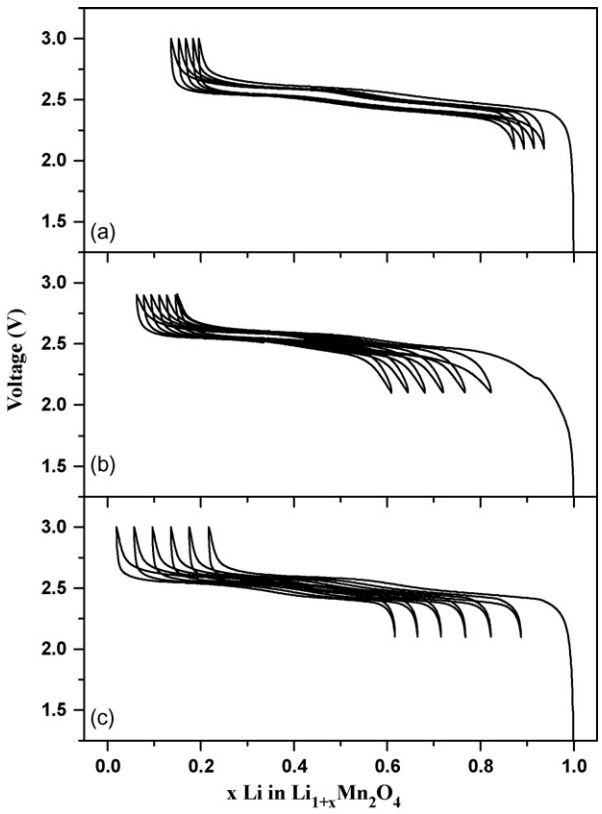

Fig. 13. Charge–discharge curves for $Li_4Ti_5O_{12}$ (PTFE)//$LiMn_2O_4$ (PTFE) full cells cycled at C/20 rate using (a) BF, (b) BFH, and (c) standard electrolytes.

the electrolyte salts employed. This range included voltages up to 4.4 V vs. Li for BF, and up to 4.6 V vs. Li for BFH and $LiPF_6$. The cell voltages were 1.8–2.9 V for BF, and 2.1–3.1 V for both BFH and the $LiPF_6$ standard.

Figs. 11 and 12 present the potential-composition profiles and capacity vs. cycle number plots of the $Li_4Ti_5O_{12}$ (cast)/BF, BFH or standard/$LiMn_2O_4$ (powder). The corresponding profiles for $Li_4Ti_5O_{12}$ (PTFE)/BF, BFH or standard/$LiMn_2O_4$ (PTFE) are depicted in Figs. 13 and 14. In all cases, the cells were cycled at a constant rate of C/20 relative to $LiMn_2O_4$. As expected from the specific characteristic of the selected anode and cathode materials, the complete cells operate with a two-slope voltage profile, averaging around 2.5 V. In addition, all cells exhibit acceptable polarization. The corresponding values for initial capacity and coulombic efficiency are given in Table 2.

The initial delivered capacity values are similar to those usually quoted in the literature [33]: 100–120 and 120–130 mAh g^{-1} for $Li_4Ti_5O_{12}$ (cast)//$LiMn_2O_4$ (powder) and $Li_4Ti_5O_{12}$ (PTFE)//$LiMn_2O_4$ (PTFE), respectively. These differences in capacity, together with the irreversible capacity in the first cycle, are certainly coming from $LiMn_2O_4$ electrodes (see Fig. 3) and could be overcome by first cycling these electrodes in half lithium cells to ensure effective

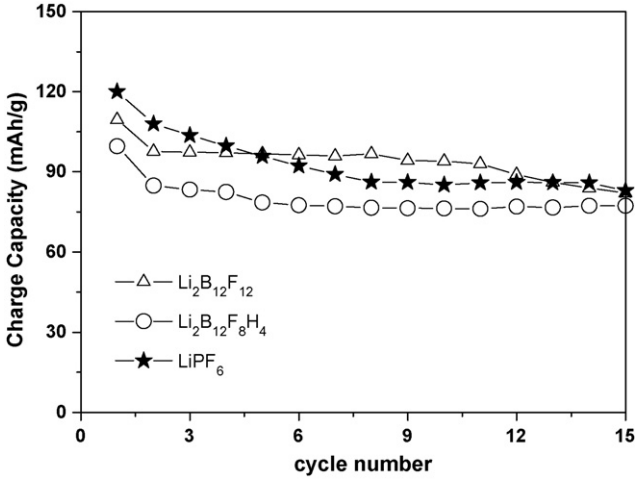

Fig. 12. Specific charge capacity vs. cycle number profiles of $Li_4Ti_5O_{12}$ (cast)//$LiMn_2O_4$ (powder) full cells cycled at C/20 rate using (a) BF, (b) BFH, and (c) standard electrolytes.

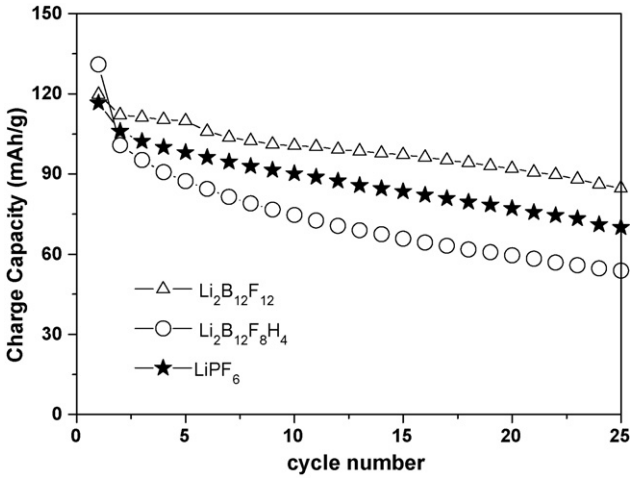

Fig. 14. Specific charge capacity vs. cycle number profiles of $Li_4Ti_5O_{12}$ (PTFE)//$LiMn_2O_4$ (PTFE) full cells cycled at C/20 rate using (a) BF, (b) BFH, and (c) standard electrolytes.

Table 2
Initial capacity and coulombic efficiency of $Li_4Ti_5O_{12}$/$LiMn_2O_4$ cells.

Electrode	Electrolyte	Initial capacity (mAh g^{-1})	Coulombic efficiency (%)/cycle number
$Li_4Ti_5O_{12}$ (cast)//$LiMn_2O_4$ (powder)	BF	110	84/15
	BFH	100	91/15
	Standard	120	77/15
$Li_4Ti_5O_{12}$ (PTFE)//$LiMn_2O_4$ (PTFE)	BF	120	76/25
	BFH	131	54/25
	Standard	117	66/25

balancing of the cells [33]. In the case of $Li_4Ti_5O_{12}$ (cast)//$LiMn_2O_4$ (powder) cells, these losses are higher, and some electrolyte degradation seems to occur for BF salts. However, the capacity retention upon cycling is quite good (Fig. 12) and, in agreement with the results obtained for half cell $Li_4Ti_5O_{12}$ cast electrode tests, reversible capacities and coulombic efficiencies seem to be slightly better for BF electrolytes.

$Li_4Ti_5O_{12}$ (PTFE)//$LiMn_2O_4$ (PTFE) cells exhibit lower irreversible capacity on the first cycle. Interestingly, an additional irreversible redox process seems to take place on the first charge, in agreement with what was observed when testing $LiMn_2O_4$ (PTFE) electrodes in half cells (Fig. 3b). For the standard $LiPF_6$ cell, there was a systematic shift of the electrochemical curve towards more negative potentials, which may be due to electrolyte decomposition. Such a reaction does not seem to take place for BFH and BF salts. As shown in Fig. 14, the capacity retention of $Li_4Ti_5O_{12}$ (PTFE)//$LiMn_2O_4$ (PTFE) cells is roughly similar for the three electrolytes. A progressive decay of the delivered capacity is also observed, fading about 1–2% per cycle. At the end of 25 charge/discharge cycles, the calculated coulombic efficiencies were estimated as follows: 76% for BF, 54% for BFH and 66% for the standard $LiPF_6$. Since these losses were not observed when separately testing the electrodes in half cells, it must be concluded that they are related to the full cell assembly. It is expected that these losses will be overcome by optimizing technological parameters such as battery configuration, electrode thickness and balancing, which are currently being tested in a separate study. Nonetheless, and in agreement with the results presented previously, the best electrochemical performance is obtained when using BF as electrolyte salt. All test results presented in this study, albeit obtained at a laboratory scale, show the beneficial properties of $Li_2B_{12}F_{12}$ and support is application as an electrolyte salt.

4. Conclusion

The main goal of this study was the investigation of the laboratory-scale electrochemical performance of two new fluorinated boron cluster lithium salts as electrolytes for $LiMn_2O_4$//$Li_4Ti_5O_{12}$ lithium-ion cells using different electrode technologies. In tests using both half cell and full cell configurations, these fluorinated cluster salts demonstrated comparable or even superior performances in terms of capacity and coulombic efficiency when compared with the standard $LiPF_6$ salt. Slightly higher polarization was observed with the new salts, however, probably due to the differences in electrolyte conductivity. Results from this study confirm that such polyfluorinated boron cluster salts are, indeed, good candidates for use in advanced, safe lithium-ion batteries. Particularly promising is $Li_2B_{12}F_{12}$, which allows delivery of highest capacity with lower polarization compared to $Li_2B_{12}F_8H_4$. The cell performance reported here can certainly be further enhanced by optimizing technological parameters and cell design.

Acknowledgment

We acknowledge MATGAS 200 AIE for the provision of their experimental facilities.

References

[1] T. Nagaura, Prog. Batt. Batt. Mater. 10 (209) (1991) 218.
[2] B.V. Ratnakumar, M.C. Smart, A. Kindler, H. Frank, R. Ewell, S. Surampudi, J. Power Sources 119 (2003) 906.
[3] C.F. Holmes, J. Power Sources 97 (2001) 739.
[4] C.L. Schmidt, P.M. Shardtad, J. Power Sources 97 (2001) 742.
[5] J.-M. Tarascon, D. Guyomard, Solid State Ionics 69 (1994) 293.
[6] D. Aurbach, Y. Ein-Eli, B. Markovsky, A. Zaban, S. Luski, Y. Carmeli, H. Yamin, J. Electrochem. Soc. 142 (1995) 2882.
[7] K. Takata, M. Morita, Y. Matsuda, J. Electrochem. Soc. 132 (1985) 126.
[8] N. Katayama, T. Kawamura, Y. Baba, J. Yamaki, J. Power Sources 109 (2002) 321.
[9] M. Ue, J. Electrochem. Soc. 142 (1995) 2577.
[10] K. Xu, Chem. Rev. 104 (2004) 10.
[11] C.W. Walker, J.D. Cox, M. Salomon, J. Electrochem. Soc. 143 (1996) L80.
[12] A. Webber, J. Electrochem Soc. 138 (1991) 2586.
[13] C. Capiglia, Y. Saito, H. Kageyama, P. Mustarelli, T. Iwamoto, T. Tabuchi, H. Tukamoto, J. Power Sources 81–82 (1999) 859–862.
[14] Y. Saito, C. Capiglia, H. Kataoka, H. Yamamoto, H. Ishikawa, P. Mustarelli, Solid State Ionics 136–137 (2000) 1161–1166.
[15] A.M. Stephan, Eur. Poly. J. 42 (2006) 21–42.
[16] S. Leroy, H. Martinez, R. Dedryvere, D. Lemordant, D. Gonbeau, Appl. Surf. Sci. 253 (2007) 4895–4905.
[17] W. Xu, C.A. Angell, Electrochem. Solid-State Lett. 4 (2001) E1.
[18] K. Xu, S.S. Zhang, U. Lee, J.L. Allen, T.R. Jow, J. Power Sources 146 (2005) 79–85.
[19] K. Kanamura, Electrolytes for lithium batteries, in: T. Nakajima, H. Groult (Eds.), Fluorinated Materials for Energy Conversion, Elsevier Ltd., 2005, pp. 253–266 (Chapter 11).
[20] S.V. Ivanov, W.J. Casteel, G.P. Pez, M. Ulman, Polyfluorinated boron cluster anions for lithium electrolytes, Patent Number: US 2,005,064,288.
[21] G. Gopalakrishnan, G. Dantsin, Z. Shi, R.M. Pearlstein, C.J. Mammarella, W.J. Casteel Jr., Air Products' StabiLife™ electrolyte salts for application in lithium ion batteries, in: International Conference: 212th Meeting of the Electrochemical Society, Washington, DC, October, 2007.
[22] J. Arai, A. Matsuo, T. Fujisaki, K. Ozawa, J. Power Sources 193 (2009) 851–854.
[23] K. Haysmizu, A. Matsuo, J. Arai, J. Electrochem. Soc. 156 (2009) A744–750.
[24] J.-M. Tarascon, W.R. McKinnon, F. Coowar, T.N. Bowmer, G. Amatucci, D. Guyomard, J. Electrochem. Soc. 141 (1994) 1421.
[25] M.R. Palacín, Y. Chabre, L. Dupont, M. Hervieu, P. Strobel, G. Rousse, C. Masquelier, M. Anne, G.G. Amatucci, J.-M. Tarascon, J. Electrochem. Soc. 147 (3) (2000) 845–853.
[26] G.J. Wang, J. Gao, L.J. Fu, N.H. Zhao, Y.P. Wu, T. Takamura, IMLB 2006, Abstract #239.
[27] G.J. Wang, J. Gao, L.J. Fu, N.H. Zhao, Y.P. Wua, T. Takamura, J. Power Sources 174 (2007) 1109–1112.
[28] J. Rodriguez-Carvajal, Physica B 192 (1993) 55–69.
[29] D. Guyomard, J.M. Tarascon, J. Electrochem. Soc. 139 (1992) 937.
[30] T. Ohzuku, A. Ueda, N. Yamamoto, J. Electrochem. Soc. 142 (1995) 1431.
[31] M.M. Tackeray, A. de Kock, M.H. Rossouw, D. Liles, J. Electrochem. Soc. 139 (1992) 363.
[32] G.G. Amatucci, J.-M. Tarascon, J. Electrochem. Soc. 149 (2002) K31.
[33] P. Reale, S. Panero, B. Scosati, J. Electrochem. Soc. 152 (10) (2005) A1949–A1954.